Biomaterials Science

Synthetic hydrogels support robust and reproducible cardiomyocyte differentiation.

Journal:	*Biomaterials Science*
Manuscript ID	BM-ART-12-2024-001636.R1
Article Type:	Paper
Date Submitted by the Author:	11-Feb-2025
Complete List of Authors:	Amitrano, Margot; University of Wisconsin-Madison Cho, Mina; University of Wisconsin-Madison Coughlin, Eva; University of Wisconsin-Madison Palecek, Sean; University of Wisconsin-Madison, Chemical and biological engineering Murphy, William; University of Wisconsin

ARTICLE

Synthetic hydrogels support robust and reproducible cardiomyocyte differentiation.

Margot J. Amitrano[a], Mina Cho[b], Eva M. Coughlin[a], Sean P. Palecek[c] and William L. Murphy[a,d]*

Received 00th January 20xx,
Accepted 00th January 20xx

DOI: 10.1039/x0xx00000x

Cardiomyocyte manufacturing from human pluripotent stem cells is limited by the variability of differentiation efficiencies, partly attributed to the widespread use of the tumor-derived substrate Matrigel. Here, we describe a screening approach to identify fully-defined synthetic PEG hydrogels that support iPSC-derived cardiac progenitor cell (iPSC-CPC) adhesion, survival, and differentiation into iPSC-derived cardiomyocytes (iPSC-CMs). Our PEG hydrogels supported superior iPSC-CM differentiation efficiency, with a 24 % increase in cTnT expression, and greater reproducibility when compared to cells cultured on Matrigel. By combining our 5-level, 3-variable full factorial screening approach with multi-variate analysis, we showed that all substrate variables manipulated here (adhesion ligand type/concentration, stiffness) had a significant influence on iPSC-CPC confluency and that iPSC-CM differentiation was significantly influenced by adhesion ligands. These results highlight the benefit of synthetic, tunable cell culture substrates and multi-variate screening studies to identify substrate formulations for a targeted cell behavior.

Introduction

Human induced pluripotent stem cells (iPSCs) can successfully be differentiated into cardiomyocytes (iPSC-CMs) [1], creating a promising supply of iPSC-CMs to regenerate the heart post-infarction or for use in disease modeling and drug screening applications [2-4]. However, iPSC-CMs are limited by their large batch-to-batch variability in differentiation efficiencies, which may be caused in part by heterogeneity in the traditional stem cell culture substrate Matrigel [5,6]. Matrigel consists of basement-membrane extracellular matrix (ECM) proteins and growth factors derived from an Englebreth-Holm-Swarm tumor formed in mice. This substrate can lead to xenogeneic contamination of cells during culture [6] and has variable composition between batches [7-9], resulting in unpredictable cell behavior [3,10]. In addition, the Matrigel shear modulus has ranged from 0.1–0.3 kPa, whereas cardiac tissue ranges from 0.5–6.0 kPa throughout heart development and can reach greater than 10 kPa during cardiac disease [4,5,11,12].

Synthetic hydrogel substrates have emerged as an alternative to Matrigel for cell culture applications [6]. For example, poly(ethylene glycol) (PEG) hydrogels are widely used as a base substrate, as they are typically bioinert, but can be readily modified to present cell adhesion ligands. Synthetic hydrogels have often been used as an experimental tool to systematically study the influence of a specific substrate chemical or mechanical property on cell behavior [13,14]. Simultaneous co-variation of multiple substrate properties has been more rarely explored, but is important to ascertain how multiple variables interact synergistically to influence a cell behavior of interest. In particular, studying multi-variate effects of substrate properties on iPSC-CM differentiation may identify substrate formulations that effectively improve upon and replace Matrigel, and maximize development of a desired cell phenotype.

PEG hydrogels have already been successful in supporting robust iPSC-CM differentiation, highlighting the material's potential as an alternative cell culture substrate. Past studies demonstrate high control over PEG hydrogel biochemical and mechanical properties and the influence of these variables on iPSC-CM culture [15-18]. These prior studies have mainly limited their focus to single variable manipulation, not taking full advantage of one of the important properties of PEG hydrogel materials: their complete tunability.

Here, we hypothesized that systematically and combinatorially varying multiple synthetic ECM properties would identify biomaterials that support adhesion, survival, and differentiation of iPSC-derived cardiac progenitor cells (iPSC-CPCs) to cardiomyocytes. The ranges of substrate parameters used here were selected to mimic aspects of human cardiac development, including stiffness ranges and prevalent types of cell adhesion ligands [19]. Our screening approach identified PEG hydrogel formulations able to support adhesion and survival of iPSC-CPCs, and showed greater iPSC-CM differentiation efficiency and reproducibility than the gold standard Matrigel substrate.

Results

Synthetic PEG hydrogels enabled control of substrate properties.

[a] Department of Biomedical Engineering, University of Wisconsin-Madison, Madison, WI USA.
[b] Department of Materials Science and Engineering, University of Wisconsin-Madison, Madison, WI USA.
[c] Department of Chemical and Biological Engineering, University of Wisconsin-Madison, Madison, WI USA.
[d] Department of Orthopedics and Rehabilitation, University of Wisconsin-Madison, Madison, WI USA.
*Corresponding author can be contacted at Wisconsin Institute for Medical Research II, 1111 Highland Avenue Room 5405, Madison, WI USA 53705. Phone: (608)265-9978; Email: wlmurphy@wisc.edu

A three-factor, five-level full factorial design was used to define the PEG hydrogel conditions which were screened for iPSC-CPC adhesion, survival, and differentiation (Fig. 1a). Using a fully defined hydrogel synthesis workflow, we developed non-degradable PEG hydrogels of varying formulations (Fig. 1b, Table S1). By manipulating the monomer-to-crosslinker ratio, we observed a high level of control over the resulting hydrogel shear modulus, with moduli ranging from 0.5 kPa (2.5 mM PEG-NB, 10 mM PEG-DT) to 10 kPa (8 mM PEG-NB, 64 mM PEG-DT). The hydrogel moduli spanned the ranges measured in previous studies for cardiac tissue at different developmental stages: < 3 kPa in a neonatal environment, 3 – 9 kPa in a healthy environment, and > 9 kPa in a fibrotic environment [19,25-28] (Fig. S1a). In addition, synthetic peptides were efficiently incorporated into the PEG hydrogels, ranging between 85 – 95 % thiols reacted across conditions (Fig. S1b). The resulting hydrogel swelling ratio from preparation to fully swollen varied with respect to the concentration of input materials, ranging between 11 – 27 % swelling across conditions (Fig. S2). The mechanical properties of the resulting PEG hydrogels were unchanged by the addition of peptides (Fig. S3), as previously demonstrated [21,29,30].

Synthetic PEG hydrogels supported iPSC-CPC adhesion and survival.

Screening 125 PEG hydrogel formulations identified 52 PEG hydrogels that supported iPSC-derived cardiac progenitor cell (iPSC-CPC) adhesion and survival (Fig. 2), defined here as greater than 20 % cell confluency, at 72 hours post-seeding. A three-variable, five-level full factorial design generated 125 initial PEG hydrogel formulations that were tested for their ability to support iPSC-CPC adhesion and survival. iPSC-CPC populations adopted distinct morphologies on different PEG hydrogel surfaces, ranging from large cell colonies to dispersed cell clusters (Fig. 2a). This observation also translated to varying confluency levels across hydrogel conditions (Fig. 2b). All PEG hydrogel conditions without an RGD peptide were unable to support cell survival, indicating that the laminin-derived peptides (IKVAV, YIGSR) alone did not support iPSC-CPC adhesion and survival at the ligand densities tested (Fig. 2c). The extent of cell dispersion on the PEG hydrogel surface also varied with the identity of the synthetic peptide (Fig. 2c, Fig. S4). The presence of c(RGDfC) resulted in higher cell confluency (Fig. S4a), reaching up to 50 % for the PEG hydrogel formulation 3.5 mM c(RGDfC) at 0.5 kPa (Fig. 2b). Cell confluency levels were also greater on substrates with lower stiffnesses, with moduli similar to those present in neonatal and healthy adult cardiac tissues (Fig. 2d). In contrast, PEG hydrogels with the highest shear modulus tested (10 kPa) had limited cell survival at 72 hours post-seeding (Fig. 2d). iPSC-CPCs on Matrigel were highly confluent, reaching 73 ± 5 % confluency, surpassing levels seen on PEG hydrogel formulations.

Properties of synthetic PEG hydrogels individually influenced iPSC-CPC confluency.

A multi-variate analysis revealed key hydrogel variables that influenced iPSC-CPC confluency levels, with a coefficient of determination of 0.43 (Fig. S5a). Both c(RGDfC) and CRGDSP peptides had a direct effect on the level of cell confluency ($p < 0.0001$ and $p < 0.01$, respectively). Higher concentrations of these two peptides resulted in greater cell confluency (Fig. 2e). Hydrogel stiffness also had a significant negative correlation with iPSC-CPC confluency ($p < 0.001$, Fig. 2e). However, the interactive effects of multiple substrate variables did not significantly influence cell confluency levels (Fig. 2e).

Synthetic PEG hydrogels supported robust levels of iPSC-CPC differentiation into cTnT+ iPSC-CMs.

PEG hydrogels supported high levels of iPSC-CPC differentiation into iPSC-CMs, regardless of substrate formulation. Due to the large number of samples, one third of the hydrogel samples (48 out of 126 conditions, with 3 replicates each) were initially selected at random to assess the overall level of differentiation (Table S2). Synthetic hydrogels supported high levels of differentiation, as 74 ± 5 % of cells on synthetic hydrogels expressed the cardiomyocyte marker cTnT (Fig. 3a). In addition, iPSC-CMs differentiated on PEG hydrogels exhibited apparently high levels of cTnT expression across the entire surface of the substrate (Fig. 3c), with robust, uniform contractility (Fig. S6). In comparison, 60 ± 11 % of cells differentiated on Matrigel expressed cTnT at an apparently lower level than the cells on PEG hydrogels (Fig. 3a-b). Further, no difference was observed across the CM markers at different steps in the differentiation (progenitor stage: NKX2.5, ISL1; differentiated stage: cTnT) for cells differentiated on PEG hydrogels, whereas we observed a significant decrease in the cell population expressing ISL1, a cardiac progenitor marker, and that expressing cTnT, a cardiomyocyte marker, for cells differentiated on Matrigel (Fig. 3c, Fig. S7, Table S3). This may indicate that PEG hydrogels supported similar iPSC-CPC adhesion as Matrigel and the increased cTnT expression on PEG hydrogels was due to a greater commitment of iPSC-CPCs to iPSC-CMs rather than a hydrogel selection of iPSC-CPCs during seeding.

In a separate experiment, we evaluated whether PEG hydrogel substrates could “rescue” a differentiation – that is, whether PEG hydrogels could improve differentiation of iPSC-CPC populations that showed poor differentiation efficiency on Matrigel. In particular, a batch of iPSC-CPCs that showed 36 ± 3 % cTnT expression when differentiated on Matrigel in one experiment, was re-seeded onto various PEG hydrogel formulations in a second experiment (Table S4). On the PEG hydrogels, the cells reached 52 ± 6 % cTnT expression across all formulations, with the best performing hydrogel formulation supporting 62 ± 12% iPSC-CM differentiation (Fig. 3d). In comparison, iPSC-CPCs reseeded onto Matrigel in the second experiment reached only 40 ± 10 % cTnT expression (Fig. 3d).

PEG hydrogel parameters influenced iPSC-CPC differentiation into iPSC-CMs.

The identity of cell adhesion peptides present in the PEG hydrogel substrates significantly influenced iPSC-CPC differentiation into iPSC-CMs (Fig. 4a, Fig. S8). A multi-variate analysis model was developed, with a coefficient of determination of 0.56 (Fig. S5b), to study the roles of these substrate parameters in iPSC-CM differentiation efficiency. The primary peptide (either c(RGDfC) or CRGDSP) correlated positively with cTnT expression ($p < 0.0001$), indicating a

strong influence of the c(RGDfC) peptide (Fig. 4b). Similarly, the secondary peptide (either CIKVAV or CYIGSR) correlated positively with iPSC-CPC differentiation into iPSC-CMs ($p < 0.01$), highlighting the importance of the CYIGSR peptide (Fig. 4b). The interactive effects of multiple substrate variables did not demonstrate a significant influence on differentiation efficiency (Fig. 4b). In addition, hydrogel stiffness, measured as shear modulus, did not have a significant influence on iPSC-CM differentiation over the range tested here (Fig. 4b). Further, an additional multi-variate analysis model, with a coefficient of determination of 0.39 (Fig. S5c), revealed the influence of both the cell number and cell confluency levels on differentiation efficiency. Both cell number and confluency level were observed to correlate positively with iPSC-CM differentiation levels ($p = 0.001$ and $p = 0.01$, respectively) (Fig. 4c), highlighting the influence of both cell-cell and cell-substrate interactions on iPSC-CM differentiation.

Synthetic PEG hydrogels supported reproducible levels of iPSC-CPC differentiation into iPSC-CMs.

iPSC-CPC differentiation levels were more reproducible on PEG hydrogels between experiments and between experimental replicates when compared to iPSC-CPC differentiation on Matrigel. Across experiments, PEG hydrogels supported a higher rate of reproducibility, measured as the standard deviation of cTnT expression (%), compared to Matrigel (Fig. 5a). The reproducibility level on PEG hydrogels was measured as an average of 48 different PEG formulations (Table S2), highlighting that the platform itself supported reproducible differentiation levels irrespective of the specific formulation. Similarly, the PEG hydrogels supported superior reproducibility to Matrigel across replicates (Fig. 5b). This highlighted the heterogeneity of Matrigel even within a single batch, as previously reported [7,8], and the relative consistency of the synthetic PEG formulations.

Discussion

Synthetic materials have proven effective in improving differentiation outcomes for several cell types, including hMSCs [31-33], endothelial cells [24,31], hepatoblasts [34,36], neural stem cells [36,37], iPSC-derived alveolar cells [38], and PSC-CMs [20,39], and outperforming the traditional Matrigel substrate. The complex and variable composition of Matrigel has had a direct influence on stem cell behavior, including on stem cell-derived cardiomyocyte differentiation [40-42]. Proteins found in Matrigel (e.g. Matrix metalloproteinase-3 and Chemokine ligand 2) and their negative influence on stem cell differentiation may contribute to limited iPSC-CM differentiation efficiency [40]. Through simultaneous variation of multiple substrate properties, our work builds upon other studies showing that synthetic materials improve iPSC-CM differentiation outcomes when compared to Matrigel [43-45]. For example, Jung et al. performed an engineering optimization to develop PEG hydrogels with full-length ECM proteins for improved iPSC-CM differentiation efficiency [15]. They demonstrated that a higher fraction of cells expressed the cardiomyocyte marker cTnT when cultured on their optimized substrate (40 mg/mL PEG and 1.15, 0.45, and 0.28 mg/mL of collagen, laminin, and fibronectin, respectively) when compared to blank PEG and PEG hydrogel crosslinked with the study's maximum concentration of each ECM protein [15]. Here, by systematic co-variation of multiple ECM properties, with ranges of ECM properties restricted to mimic some aspects of human cardiac development, we identified PEG hydrogel conditions relevant for iPSC-CM differentiation and compared our material to Matrigel, the traditional substrate in iPSC-CM differentiations [20]. Further, we observed a clear increase in iPSC-CM differentiation efficiency across all the PEG hydrogel formulations (Fig. 3a), highlighting the direct advantage of using synthetic PEG hydrogels relative to Matrigel.

In the context of other synthetic alternatives, we observed significantly improved cTnT expression on our PEG hydrogels (75 %) compared to other synthetic hydrogels (< 70 %) (Table 1). Recombinant ECM protein coatings performed better than synthetic hydrogels, including our PEG hydrogels. However, our best performing PEG hydrogel formulation (7 mM cRGDfC 10 kPa) demonstrated similar cTnT expression (82 %) as recombinant ECM proteins (> 80 %) (Table 1). It is worth noting that our PEG hydrogels could be further modified to potentially support greater iPSC-CM differentiation levels, which would be more challenging using recombinant ECM proteins. Overall, our PEG hydrogels outperformed other synthetic hydrogel alternatives and reached levels generally associated with recombinant ECM proteins.

Direct comparisons of iPSC-CM differentiation efficiency between different culture protocols are rare and generally do not include many synthetic alternatives. When studying the effect of synthetic materials on iPSC-CM differentiation, studies seem to focus the optimization within their respective material rather than directly comparing to the traditional iPSC-CM culture substrate Matrigel [15,16]. In addition, studies comparing iPSC-CM differentiation efficiencies across different differentiation strategies generally limit the synthetic alternatives to Synthemax or recombinant ECM proteins [46,47]. Still, Sung et al. demonstrated approximately 87 % cTnT-expressing cells on Synthemax compared to 75 % on Matrigel, resulting in a 16 % increase in cTnT expression on Synthemax [47]. Here, we demonstrated a 25 % increase in cTnT expression on our PEG hydrogels, as summarized in Table 2. We also emphasize that this is a limited description of our results as we described improvements in cTnT expression across the PEG hydrogel platform as a whole, rather than a single optimized PEG hydrogel formulation. This points to a dramatic increase in iPSC-CM differentiation efficiency on our PEG hydrogels, with potentially consequential results on iPSC-CM manufacturing.

Although high efficiency iPSC-CM differentiation is achievable via traditional methods (i.e. culture on the Matrigel substrate or other ECM-derived proteins) [1,20], differentiation efficiencies are highly variable across replicates and batches [48]. The variability in differentiation efficiencies is often attributed to the complexity and lack of compositional reproducibility in the Matrigel substrate, despite extensive quality testing required of this material to validate its ability to support iPSC culture and CM differentiation [6,9]. Notably, Matrigel mechanical and biochemical properties have been

highlighted for their lack of reproducibility, as seen through highly variable elastic modulus [8] and protein composition [40]. Matrigel variability may directly translate into variability in cell behavior, including in cell differentiation [40,49]. We have reasoned that synthetic materials, which are fully defined and tunable, could potentially minimize the variability in differentiation outcomes. Extensive characterization and use of fully-defined components in synthetic materials has been shown to contribute to superior reproducibility of other cell culture results [6,48]. For instance, a previous study showed greater reproducibility of endothelial network formation by HUVECs and iPSC-derived endothelial cells when using PEG-based hydrogels when compared to Matrigel [24]. Reproducible endothelial network formation also led to superior sensitivity and reproducibility of an endothelial "tubulogenesis" assay commonly used to evaluate angiogenesis regulators [24]. In the current study we used the same materials, at different ratios, to achieve greater reproducibility in iPSC-CM differentiation efficiency on PEG-based hydrogels (Fig. 5). Specifically, we observed a 44 % decrease in variability of cTnT expression across experimental replicates of PEG hydrogel conditions compared to Matrigel and, similarly, a 68 % decrease in variability across experiments (Fig. 5, Table 1). This suggests that these cells could also have greater value in cardiac disease modelling.

By varying multiple substrate properties simultaneously, we observed the emergence of synergies between the effects of different hydrogel properties. Although our PEG hydrogels broadly outperformed Matrigel regardless of the formulation, multi-variate analysis revealed the significant influence of the fibronectin- and laminin-derived peptides on iPSC-CM differentiation (Fig. 4b). This observation aligns with previous studies highlighting the importance of multiple ECM proteins, such as collagen, laminin, and fibronectin, in iPSC-CM differentiation [45,51,52]. For example, the significance of laminin in iPSC-CM differentiation was observed in a previous multivariate model [15]. Jung et al. showed that the ECM proteins studied were positive in maximizing cTnT expression [15], as was the case in our multivariate model showing a positive correlation between cTnT expression and the synthetic cell adhesion peptides tested (Fig. 4b). Further, Jung et al. highlighted that laminin had the most significant main effect on differentiation when compared to collagen and fibronectin [15]. In comparison, we showed that the c(RGDfC) and CRGDSP peptides have an integral role in the iPSC-derived CPC-to-CM differentiation (Fig. 4b), possibly indicating that the role of the RGD peptide motif (fibronectin-derived) is greater during terminal differentiation from progenitor to cardiomyocyte. Neiman et al. showed increased expression of fibronectin at the CPC stage, compared to the undifferentiated stage. The cell integrin receptor subunit α5 engaged by fibronectin was also shown to be up-regulated at the CPC stage [53]. Similarly as in our work, fibronectin appeared to have a crucial role at the CPC stage of iPSC-CM differentiation [53]. Further, we showed the importance of c(RGDfC) and CRGDSP peptides for cell confluency (Fig. 2e). The increased level of cell confluency may have contributed to improvements in iPSC-CM differentiation. Although substrate stiffness, measured as the shear modulus, has been previously shown to influence iPSC-CM differentiation [10,11], it had a minimal influence here in comparison to the influence of ECM-derived cell adhesion peptides (Fig.4b). This may be caused by the relatively small range of shear modulus assessed here, as substrate stiffness can be varied over a much larger range of moduli (100s of kPa) [48] but was limited here in order to remain within physiologically relevant cardiac stiffnesses [7,8,10,11]. Cell adhesion ligands played an apparently more significant role in iPSC-CPC differentiation into iPSC-CMs compared to substrate stiffness (Fig. 4b).

We showed that individual substrate variables directly influenced iPSC-CM differentiation efficiency whereas combinatorial effects were not significant (Fig. 4b). This highlights the apparently independent roles of substrate stiffness and cell adhesion ligands on iPSC-CPC differentiation into iPSC-CMs in the context of our experimental parameter space. The individual influence of fibronectin and laminin proteins was previously observed by Jung et al., and their combination demonstrated a lesser effect [15]. Specifically, collagen and laminin had a significant influence on expression of the cardiomyocyte marker cTnT, with fibronectin having a less significant role, while all interaction effects between distinct proteins did not significantly influence cTnT expression. Here, we similarly showed a stronger influence of individual substrate variables when compared to interactive effects (Fig. 4b).

Materials and Methods

iPSC culture and maintenance

WTC11 human iPSCs were maintained on 6-well plates coated with Matrigel (Corning) in mTeSR medium (Stem Cell Technologies) at 37°C and 5% CO_2. The media was changed every day and cells were passaged every 3 days using Versene (Life Technologies) for transfer to fresh Matrigel-coated plates.

iPSC-CM differentiation

iPSCs were differentiated to cardiomyocytes as previously described [20]. Briefly, stem cells were passaged to a fresh Matrigel-coated 12-well plate using Accutase (Sigma Aldrich) and seeded at 40,000 cells/cm^2 in mTeSR medium with 5 uM ROCK inhibitor (R&D Systems). Cells were expanded for 2 days with daily changes of mTeSR medium. On day 0 of differentiation, the media was changed to RPMI 1640 medium (Thermo Fisher Scientific) with B27 supplement without insulin (B27-; Thermo Fisher Scientific), supplemented with 7 uM CHIR-99021 (Selleck Chemicals), to induce differentiation. After 48 hours, cells were fed with fresh RPMI 1640 medium with B27- supplemented with 5 uM IWP2 (Tocris). After an additional 48 hours, cells were then fed with fresh RPMI 1640 medium with B27-. On day 6 of differentiation, the media was replaced with fresh RPMI 1640 medium with B27 supplement with insulin (B27+; Thermo Fisher Scientific). Cells were then fed with RPMI 1640 medium with B27+ every 2-3 days until day 16 of differentiation. Initial steps of the differentiation were conducted on Matrigel until the cardiac progenitor stage (day 5 of differentiation), at which point the cells were lifted and singularized using Accutase

and frozen in liquid nitrogen. Cells were then thawed and seeded either on Matrigel or PEG hydrogels for continued differentiation.

PEG hydrogel synthesis

PEG hydrogels were prepared using 8-arm, 20 kDa norbornene-functionalized PEG (JenKem Technology), 3.4 kDa PEG di-thiol (Laysan Bio) crosslinker, 0.1 wt/wt% Irgacure 2959 (CIBA) photoinitiator, diluted with DPBS (Gibco) to reach desired concentrations. The following peptides were added at varying concentrations: CRGDSP (3.5 mM or 7 mM) or head-to-tail cyclized RGDfC (cRGDfC, where the "f" notation represents a D-amino acid; 3.5 mM or 7 mM), referred to as a primary peptide, and CIKVAV (1.5 mM or 3 mM) or CYIGSR (1.5 mM or 3 mM), referred to as a secondary peptide. All peptides were purchased from GenScript. The shear modulus of the hydrogels was varied by adjusting the monomer-to-crosslinker ratio. We assayed physiologically relevant stiffnesses, measured as shear modulus, corresponding to neonatal (0.5 kPa and 2 kPa), healthy adult (4 kPa and 6 kPa), and fibrotic (10 kPa) cardiac tissue [4,5,11,12]. A full factorial design of these 3 variables (primary peptide, secondary peptide, and shear modulus) was used to define the hydrogel formulations tested here.

Hydrogel shear modulus was characterized using methods previously described [21-25]. Shear modulus was tested on bulk hydrogel samples demonstrating dimensions of 8.0 mm diameter and 1.2 mm depth. Hydrogels were incubated in PBS for 24 hours to allow swelling prior to testing. The Ares-LS2 rheometer (TA Instruments) was used to test hydrogel shear modulus. Parallel plates of the same dimensions as our hydrogel samples were used to apply a 20 g force. A dynamic strain sweep test with 1 Hz frequency was performed between 0.1 and 50 % strain. The shear modulus for each sample was measured between 1 to 10 % strain.

Peptide incorporation into the hydrogel during polymerization was assessed using methods previously described [21-25]. Briefly, the availability of free thiol groups was measured using the Ellman's assay (Thermo Fisher Scientific). After hydrogel polymerization, the gels were incubated in Ellman's buffer for 20 minutes. Absorbance was read on a plate reader at 412 nm. A standard curve using L-Cysteine hydrochloride was used to measure remaining thiol content in the hydrogel.

Confluency characterization

Cells were imaged on day 3 after seeding to assess confluency levels. Samples were stained by washing with PBS and incubating in RPMI 1640 medium with B27+, containing 1.5 uM ethidium homodimer-1 and 1 uM calcein-AM (Thermo Fisher Scientific), for 30 minutes at 37°C. Samples were imaged on a Nikon TI Eclipse microscope. Samples were washed twice with PBS before adding fresh RPMI 1640 medium with B27+ supplement, for continued differentiation. Using FIJI, confluency levels were determined by thresholding fluorescence intensity and quantifying total object area per sample.

Flow cytometry

Cardiomyocyte purity was assessed using flow cytometry to measure cardiac troponin T (cTnT) expression for cells after 11 days of culture. Cells were lifted and singularized with Accutase before transferring to tubes containing DMEM/F12 medium (Thermo Fisher Scientific). Samples were centrifuged at 200xg for 5 minutes and cells were resuspended in 1% formaldehyde solution and incubated in the dark for 20 minutes at room temperature. Samples were centrifuged and resuspended in 90% methanol solution in the dark for 20 minutes at 4°C before being transferred to -20°C until processing. Samples were washed twice in Flow Buffer 1 (PBS containing 0.5 % BSA) and incubated overnight at 4°C in Flow Buffer 2 (PBS containing 0.5% BSA and 0.1% Triton X-100) with a primary antibody. Samples were then washed with Flow Buffer 2, incubated for 30 minutes at room temperature in the dark in Flow Buffer 2 with a secondary antibody, washed with Flow Buffer 2, and resuspended in Flow Buffer 1. Data was collected on an Attune flow cytometer (Thermo Fisher Scientific) and analyzed on FCS Express software. The primary antibodies used were mouse anti-human cardiac troponin T (cTnT; Abcam, 1:800), mouse anti-human ISL-1 (DSHB, 1:20), and goat anti-human NKX2.5 (Abcam, 1:100). The secondary antibodies used were donkey anti-mouse AlexaFluor 488 (Thermo Fisher Scientific, 1:1000) and donkey anti-rabbit AlexaFluor 647 (Thermo Fisher Scientific, 1:1000).

Immunofluorescence imaging

Images of cardiomyocytes were taken after 11 days in culture. Briefly, cells were fixed by incubating in 4 % formaldehyde solution for 20 minutes in the dark. After washing, fresh PBS was added and samples were placed at 4°C until staining. Samples were incubated in Flow Buffer 2 for 1 hour at room temperature, followed by an overnight incubation in Flow Buffer 2 with primary antibodies at 4°C. The samples were washed with PBS three times for 10 minutes before incubating in Flow Buffer 2 with secondary antibodies for 1 hour in the dark at room temperature. The samples were then washed an additional three times for 10 minutes before adding fresh PBS and placing samples at 4°C until imaging. Images were taken using the TI Eclipse microscope (Nikon). The primary antibody used was mouse anti-human cTnT (Abcam, 1:200). The secondary antibody used was donkey anti-mouse AlexaFluor 488 (1:1000). DAPI was used for nuclear staining (Thermo Fisher Scientific, 1:1000).

Data analysis and statistics

Multi-variate analysis was performed using JMP statistical analysis software. A standard least squares model was generated and Student t-test was performed to assess the effect of each culture parameter on the measured outcome (e.g. cell confluency, differentiation efficiency). Additional statistical analysis was performed using GraphPad Prism software with Student t-test or one-way ANOVA as indicated.

Conclusion

Efficient manufacturing of human iPSC-derived cells is highly dependent on the cell culture substrate and its ability to support effective and reproducible differentiation. Here, we identified fully-defined, xeno-free, PEG-based hydrogels as an alternative to Matrigel for human iPSC-CM differentiation. The tunability of this

technology offered a range of formulations that supported iPSC-CPC survival and iPSC-CM differentiation levels that outperformed those seen on Matrigel, while also providing significantly enhanced reproducibility. The screening approach employed here is generalizable to other cell types and could aid in identifying key environmental variables for specific human stem cell applications.

Conflicts of interest

Disclosure statement: W.L.M. is a co-founder and equity owner in Stem Pharm, Inc., which develops hydrogels for stem cell related applications. The other authors have no conflicts of interest to disclose.

Acknowledgements

This material is based upon work supported by the National Science Foundation (EEC-1648035 and DMR-2207275). The authors thank the University of Wisconsin Carbone Cancer Center Flow Cytometry Laboratory, supported by P30 CA014520, for use of its facilities and services. The authors gratefully acknowledge use of facilities and instrumentation at the UW-Madison Wisconsin Centers for Nanoscale Technology (wcnt.wisc.edu) partially supported by the NSF through the University of Wisconsin Materials Research Science and Engineering Center (DMR-1720415). Figures were created in part through www.biorender.com.

References

1 C. L. Mummery, J. Zhang, E.S. Ng, D.A. Elliott, A.G. Elefanty and T.J. Kamp, *Circulation research*, 2012, **111**, 344–358.
2 D.T. Paik, M. Chandy and J.C. Wu, *Pharmacological reviews*, 2020, **72**, 320-342.
3 S. Kussauer, R. David and H. Lemcke, *Cells*, 2019, **8**, 1331.
4 A.P. Hnatiuk, F. Briganti, D.W. Staudt and M. Mercola, *Cell chemical biology*, 2021, **28**, 271-282.
5 H.K. Kleinman and G.R. Martin, *Seminars in cancer biology*, 2005, **15**, 378-386.
6 E.A. Aisenbrey and W.L. Murphy, *Nature reviews materials*, 2020, **5**, 539-551.
7 C.S. Hughes, L.M. Postovit and G.A. Lajoie, *Proteomics*, 2010, **10**, 1886-1890.
8 J. Reed, W.J. Walczak, O.N. Petzold and J.K. Gimzewski, *Lagmuir: the ACS journal of surfaces and colloids*, 2009, **25**, 36-39.
9 S.S. Soofi, J.A. Last, S.J. Liliensiek, P.F. Nealey and C.J. Murphy, *Journal of structural biology*, 2009, **167**, 216-219.
10 S. Vukicevic, H.K. Kleinman, F.P. Luyten, A.B. Roberts, N.S. Roche and A.H. Reddi, *Experimental cell research*, 1992, **202**, 1-8.
11 A.J. Engler, C. Carag-Krieger, C.P. Johnson, M. Raab, H.Y. Tang, D.W. Speicher, J.W. Sanger, J.M. Sanger and D.E. Discher, *Journal of cell science*, 2008, **121**, 3794-3802.
12 A.J. Ribeiro, Y.S. Ang, J.D. Fu, R.N. Rivas, T.M. Mohamed, G.C. Higgs, D. Srivastava and B.L. Pruitt, *Proceedings of the National Academy of Sciences of the United States of America*, 2015, **112** 12705-12710.
13 J.G. Jacot, H. Kita-Matsuo, K.A. Wei, H.S. Chen, J.H. Omens, M. Mercola and A.D. McCulloch, *Annals of the New York Academy of Sciences*, 2010, **1188**, 121-127.
14 L.B. Hazeltine, C.S. Simmons, M.R. Salick, X. Lian, M.G. Badur, W. Han, S.M. Delgado, T. Wakatsuki, W.C. Crone, B.L. Pruitt and S.P. Palecek, *International journal of cell biology*, 2012, **2012**, 508294.
15 J.P. Jung, D. Hu, I.J. Domian and B.M. Ogle, *Scientific reports*, 2015, **5**, 18705.
16 J. Jia, R.C. Coyle, D.J. Richards, C.L. Berry, R.W. Barrs, J. Biggs, C. James Chou, T.C. Trusk and Y. Mei, *Acta biomaterialia*, 2016, **45**, 110–120.
17 K. Shapira-Schweitzer and D. Seliktar, *Acta biomaterialia*, 2007, **3**, 33–41.
18 C. Crocini, C.J. Walker, K.S. Anseth and L.A. Leinwand, *Progress in biophysics and molecular biology*, 2020, **154**, 71–79.
19 I.L. Chin, L. Hool and Y.S. Choi, *Biomaterials science*, 2021, **9**, 6795-6806.
20 X. Lian, J. Zhang, S.M. Azarin, K. Zho, L.B. Hazeltine, X. Bao, C. Hsaio, T.J. Kamp and S.P. Palecek, *Nature protocols*, 2013, **8**, 162-175.
21 N.N.T. Le, S. Zorn, S.K. Schmitt, P. Gopalan and W.L. Murphy, *Acta biomaterialia*, 2016, **34**, 93-103.
22 E.H. Nguyen, M.R. Zanotelli, M.P. Schwartz and W.L. Murphy, *Biomaterials*, 2014, **35**, 2149=2161.
23 M. Parlato, S. Reichert, N. Barney and W.L. Murphy, *Macromolecular bioscience*, 2014, **14**, 687=698.
24 E.H. Nguyen, W.T. Daly, N.N.T. Le, M. Farnoodian, D.G. Belair, M.P. Schwartz, C.S. Lebakken, G.E. Ananiev, M.A. Saghiri, T.B. Knudsen, N. Sheibani and W.L. Murphy, *Nature biomedical engineering*, 2017, **1**, 0096.
25 M. Krieg, Y. Arboleda-Estudillo, P.H. Puech, J. Käfer, F. Graner, D.J. Müller and C.P. Heisenberg, *Nature cell biology*, 2008, **10**, 429-436.
26 T.J. Herron, A.M. Rocha, K.F. Campbell, D. Ponce-Balbuena, B.C. Willis, G. Guerrero-Serna, Q. Liu, M. Klos, H. Musa, M. Zarzoso, A. Bizy, J. Furness, J. Anumonwo, S. Mironov and J. Jalife, *Arrythmia and electrophysiology*, 2016, **9**, e003638.
27 J.L. Young and A.J. Engler, *Biomaterials*, 2011, **32**, 1002-1009.
28 M.F. Berry, A.J. Engler, Y.J. Woo, T.J. Pirolli, L.T. Bish, V. Jayasankar, J.J. Morine, T.J. Gardner, D.E. Discher and J.L. Sweeney, *American journal of physiology. Heart and circulatory physiology*, 2006, **290** H2196-H2203.
29 M.W. Toepke, N.A. Impellitteri, J.M. Theisen and W.L. Murphy, *Macromolecular materials and engineering*, 2013, **298**, 699-703.
30 T.D. Hansen, J.T. Koepsel, N.N. Le, E.H. Nguyen, S. Zorn, M. Parlato, S.G. Loveland, M.P. Schwartz and W.L. Murphy, W. L, *Biomaterials science*, 2014, **2**, 745-756.
31 B.J. Klotz, L.A. Oosterhoff, L. Utomo, K.S. Lim, Q. Vallmajo-Martin, H. Clevers, T.B.F. Woddfield, A.J.W.P. Rosenberg, J. Malda, M. Ehrbar, B. Spee and D. Gawlitta, *Advanced healthcare materials*, 2019, **8**, e1900979.
32 J.T. Koepsel, P.T. Brown, S.G. Loveland, W.J. Li and W.L. Murphy, *Journal of materials chemistry*, 2012, **22** 19474-19481.
33 A.K. Patel, M.W. Tibbit, A.D. Celiz, M.C. Davies, R. Langer, C. Denning, M.R. Alexander and D.G. Anderson, *Current opinion in solid state and materials science*, 2016, **20**, 202-211.
34 Y. Zhang, A. Guo, C. Lyu, R. Bi, Z. Wu, W. Li, P. Zhao, Y. Niu, J. Na, J.J. Xi and Y. Du, *iScience*, 2021, **24**, 103303.
35 T. Yamazoe, N. Shiraki, M. Toyoda, N. Kiyokawa, H. Okita, Y. Miyagawa, H. Akutsu, A. Umezawa, Y. Sasaki, K. Kume and S. Kume, *Journal of cell science*, 2013, **126** 5391-5399.
36 S. Koutsopoulos and S. Zhang, *Acta biomaterialia*, 2013, **9**, 5162-5169.
37 D.G. Anderson, D. Putnam, E.B. Lavik, T.A. Mahmood and R. Langer, *Biomaterials*, 2005, **26**, 4892–4897.
38 C. Loebel, A.I. Weiner, M.K. Eiken, J.B. Katzen, M.P. Morley, V. Bala, F.L. Cardenas-Diaz, M.D. Davidson, K. Shiraishi, M.C.

Basil, L.T. Ferguson, J.R. Spence, M. Ochs, M.F. Beers, E.E. Morrisey, A.E. Vaughan and J.A. Burdick, *Advanced materials*, 2022, **34**, e2202992.
39 D.G. Anderson, D. Levenberg and R. Langer, *Nature* biotechnology, 2004, **22**, 863–866.
40 N.C. Talbot and T.J. Caperna, *Cytotechnology*, 2015, **67**, 873-883.
41 S. Hong, J.K. Kang, J.J. Park, E.S. Ryu, S.S. Choi, S.H. Lee, J.H. Lee and J.S. Seo, *International journal of cardiology*, 2010, **141**, 49-60.
42 Y. Tamura, K. Matsumura, M. Sano, H. Tabata, K. Kimura, M. Ieda, T. Arai, Y. Ohno, H. Kanazawa, S. Yuasa, R. Kaneda, S. Makino, K. Nakajima, H. Okano and K. Fukuda, *Arteriosclerosis, thrombosis, and vascular biology*, 2011, **31**, 582-589.
43 A.W. Smith, J.D. Hoyne, P.K. Nguyen, D.A. McCreedy, H. Aly, I.R. Efimov, S. Rentschler and D.L. Elbert, *Biomaterials*, 2013, **34**, 6559-6571.
44 C. Paoletty, C. Divieto and V. Chiono, *Cells*, 2018, **7**, 114.
45 S. Sa, L. Wong and K.E. McCloskey, *BioResearch open access*, 2014, **3**, 150-161.
46 D.M. Lyra-Leite, O. Gutiérrez-Gutiérrez, M. Wang, Y. Zhou, L. Cyganek and P.W. Burridge, *STAR Protocols*, 2022, **3**, 101560.
47 T.C. Sung, C.H. Liu, W.L. Huang, Y.C. Lee, S.S. Kumar, Y. Chang, Q.D. Ling, S.T. Hsu and A. Higuchi, *Biomaterials* science, 2019, **7**, 5467-5481.
48 S.M. Biendarra-Tiegs, F.J. Secreto and T.J. Nelson, *Cell Biology and Translational Medicine*, 2019, **6**, 1212.
49 N.T. Kohen, L.E. Little and K.E. Healy, *Biointerphases*, 2009, **4**, 69-79.
50 W.L. Murphy, McDevitt, T.C. and A.J. Engler, *Nature materials*, 2014, **13**, 547-557.
51 J. Zhang, Z.R. Gregorich, R. Tao, G.C. Kim, P.A. Lalit, J.L. Carvalho, Y. Markandeya, D.F. Mosher, S.P. Palecek and T.J. Kamp, *eLife*, 2022, **11**, e69028.
52 S.J. DePalma, C.D. Davidson, A.E. Satis, A.S. Helms and B.M. Baker, *Biomaterials science*, 2021, **9**, 93-107.
53 G. Neiman, M.A. Scarafía, A. La Greca, N.L. Santín Velazque, X. Garate, A. Waisman, A.M. Möbbs, T.H. Kasai-Brunswick, F. Mesquita, D. Martire-Greco, L.N. Moro, C. Luzzani, A. Bastos Carvalho, G.E. Sevlever, A. Campos de Carvalho, A.S. Guberman and S.G. Miriuka, *Scientific reports*, 2019, **9**, 18077.
54 P.W. Burridge, E. Matsa, P. Shukla, Z.C. Lin, J.M. Churko, A.D. Ebert, F. Lan, S. Diecke, B. Huber, N.M. Mordwinkin, J.R. Plews, O.J. Abilez, B. Cui, J.D. Gold and J.C. Wu, *Nature methods*, 2014, **11**, 855-860.
55 Y. Lin and J. Zou, *STAR protocols*, 2020, **1**, 100015.
56 Y, Tan, P. Han, Q. Gu, G. Chen, L. Wang, R. Ma, J. Wu, C. Feng, Y. Zhang, L. Wang, B. Hu, W. Li, J. Hao and Q. Zhou, *Journal of tissue engineering and regenerative* medicine, 2018, **12**, 153-163.
57 L.B. Hazeltine, M.G. Badur, X. Lian, A. Das, W. Han and S.P. Palecek, *Acta biomaterialia*, 2014, **10**, 604-612
58 A. Körner, M. Mosqueira, M. Hecker and N.D. Ullrich, *Frontiers in physiology*, 2021, **12**, 710619.

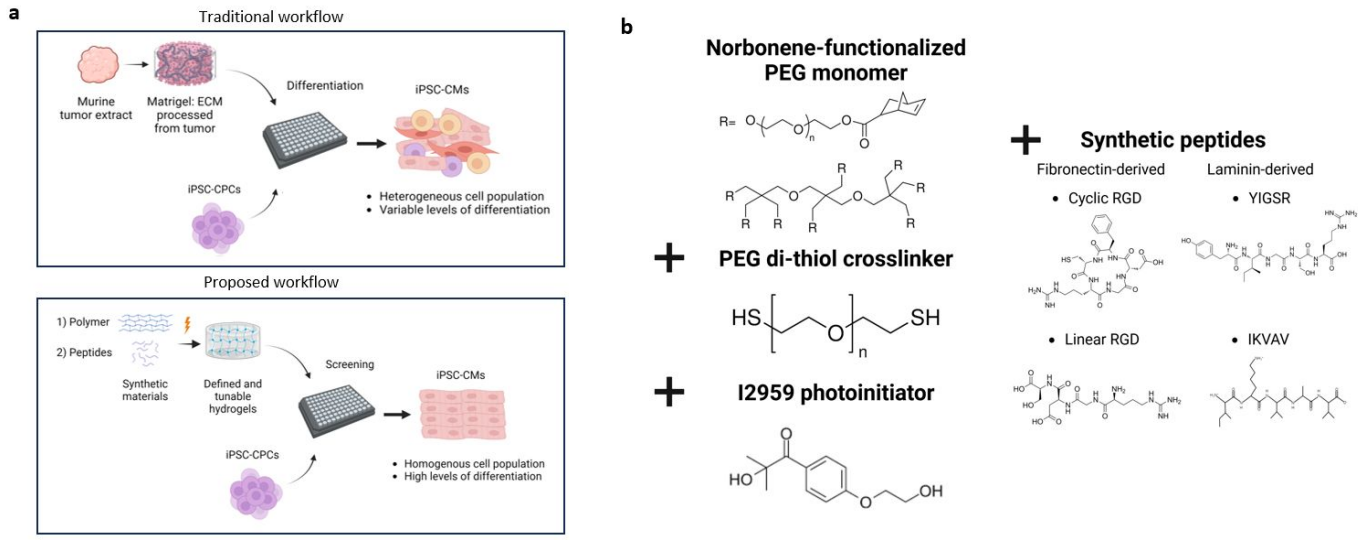

Figure 1. Schematic representation of (**a**) the traditional workflow and our proposed workflow relying on screening of PEG hydrogel formulations, and (**b**) the PEG hydrogel synthesis workflow. Schematic not to scale.

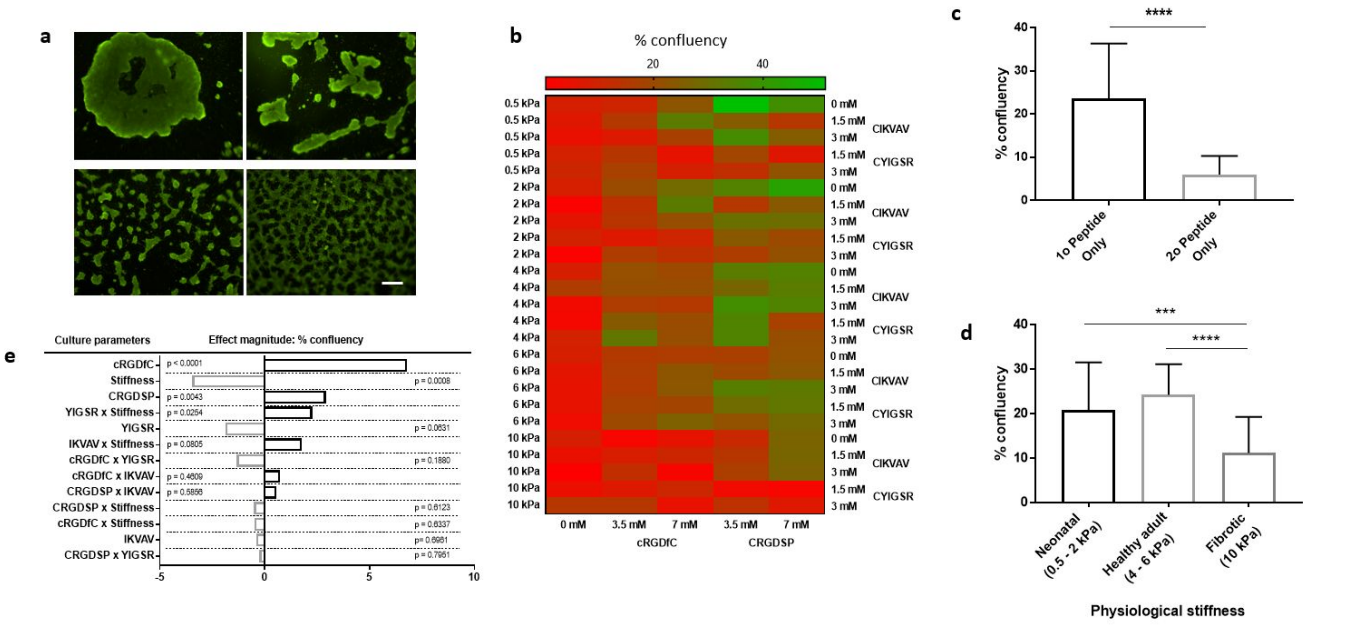

Figure 2. Synthetic PEG hydrogels, representative of developmental stages of the cardiac ECM, supported iPSC-CPC adhesion and survival. (**a**) Representative calcein-AM fluorescence images of live iPSC-CPCs cultured on PEG hydrogels 3 days after seeding. Scale bar = 500 µm. (**b**) Quantitative heat map of iPSC-CPC confluency levels at 72 hours post-seeding on PEG hydrogels. Each box = 3 replicate gels. (**c**) Confluency quantification of iPSC-CPCs cultured on PEG hydrogels presenting different peptides. **** p<0.0001, Student t-test. Each bar = 25 gels. (**d**) Confluency quantification of iPSC-CPCs cultured on PEG hydrogels with different stiffnesses. *** p<0.001, one-way ANOVA. Each bar = 50 gels (neonatal & healthy adult) or 25 gels (fibrotic). (**e**) Multivariate analysis (MVA) of individual and interactive effects of hydrogel variables on iPSC-CPC confluency levels.

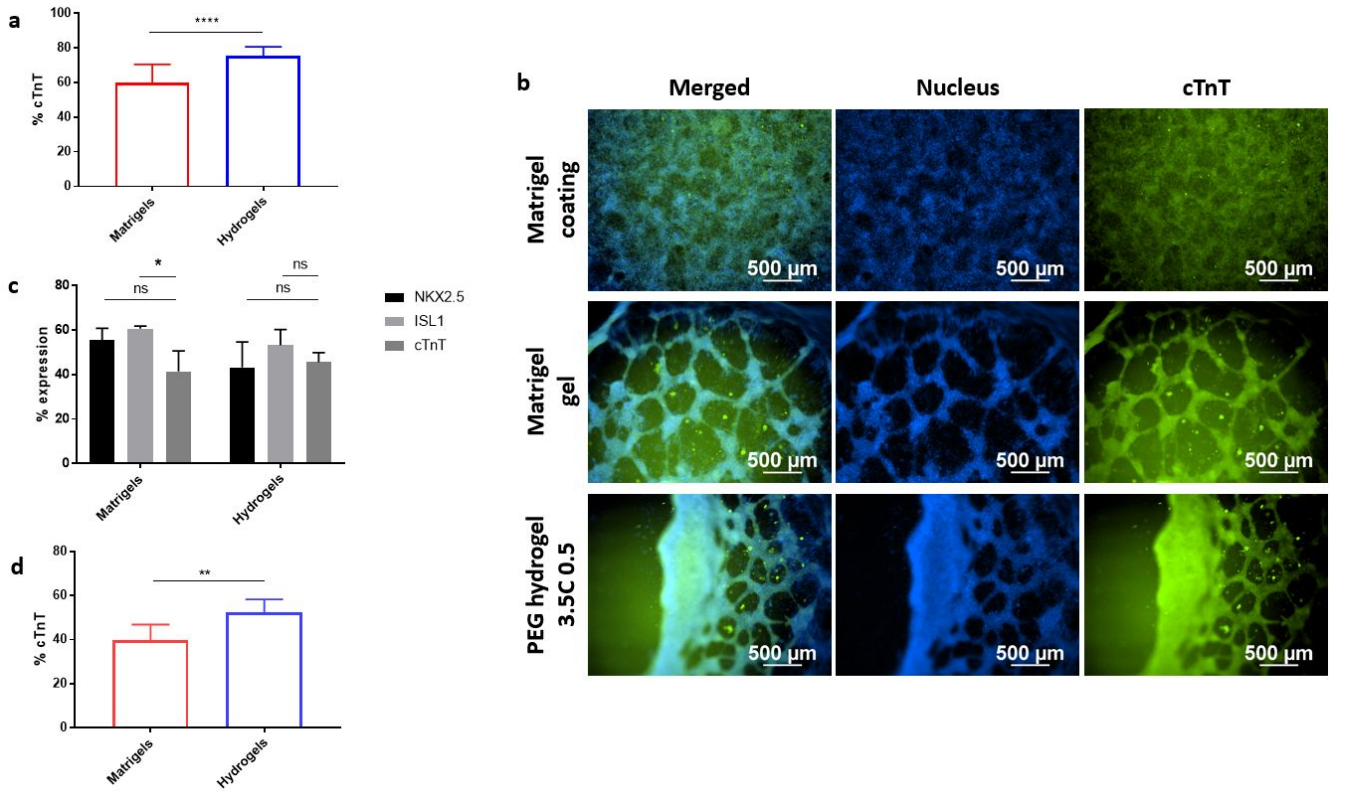

Figure 3. PEG hydrogels supported high levels of iPSC-CM differentiation. (**a**) Flow cytometry quantification of cTnT-expressing cells (%) with terminal differentiation conducted on Matrigel or PEG hydrogels. **** p<0.0001, Student t-test. Each bar = 9 gels (Matrigel) or 126 gels (PEG hydrogels). (**b**) Flow cytometry quantification of CPC markers (NKX2.5, ISL1) and CM markers (cTnT) on Matrigel and PEG hydrogels. ns: no significance, * p<0.05, one-way ANOVA. Each bar = 6 gels (Matrigel) or 9 gels (PEG hydrogels). (**c**) Immunofluorescence images of iPSC-CMs on different substrates. (**d**) Flow cytometry quantification of cTnT-expressing cells (%) rescued for terminal differentiation on PEG hydrogels or Matrigel. ** p<0.01, Student t-test. Each bar = 9 gels (Matrigel) or 44 gels (PEG hydrogels). Scale bar = 500 µm.

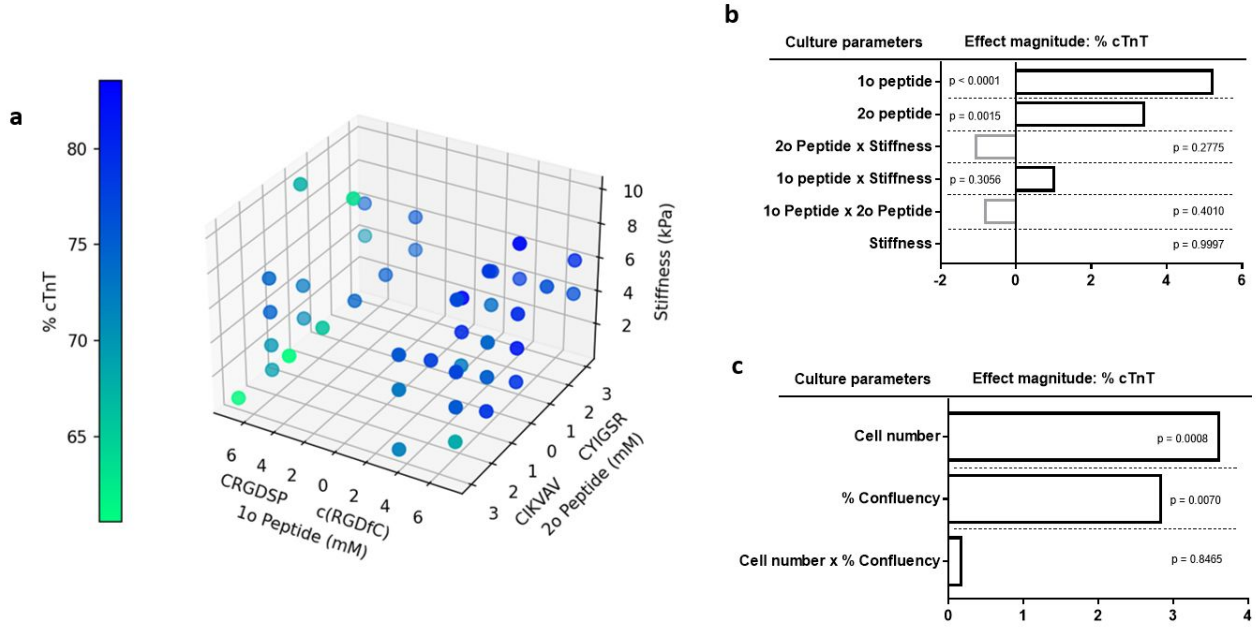

Figure 4. PEG hydrogel formulations influenced iPSC-CM differentiation efficiency. (**a**) 3D plot representative of cTnT-expressing cells (%) in PEG hydrogel formulations of varying primary peptide (0-7 mM CRGDSP, represented as negative values, or 0-7 mM c(RGDfC)), secondary peptide (0-3 mM CIKVAV, represented as negative values, or 0-3 mM CYIGSR), and stiffness (0.5-10 kPa). Each dot = 3 replicate gels. (**b**) MVA of individual and interactive effects of hydrogel variables on iPSC-CM differentiation levels. (**c**) MVA of cell number and confluency level effects on iPSC-CM differentiation levels.

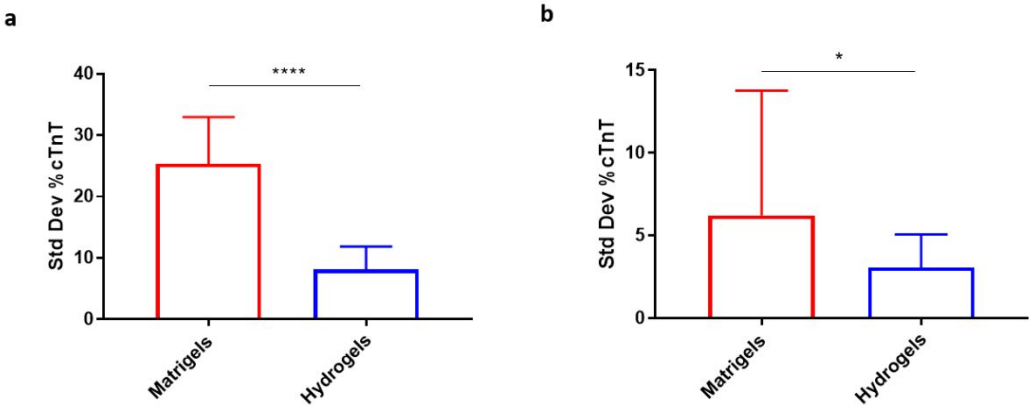

Figure 5. PEG hydrogels supported superior reproducibility in iPSC-CM differentiation efficiencies when compared to Matrigel (**a**) between experiments, **** p<0.0001, Student t-test, each bar = 3 experiments for 3 conditions (Matrigel) or 42 conditions (PEG hydrogels); and (**b**) between experimental replicates, * p<0.05, Student t-test, each bar = 3 replicates for 3 conditions (Matrigel) or 42 conditions (PEG hydrogels).

Material	cTnT expression (%)	References
Synthemax	85-95	Burridge et al. Lin et al. Sung et al.
Vitronectin	80	Tan et al. Lin et al.
Laminin	85	Burridge et al. Zhang et al.
Polyacrylamide hydrogel	70	Hazeltine et al.
Polydimethylsiloxane hydrogel	70	Korner et al.
PEG hydrogels	35	Jung et al.
Our PEG hydrogels	75	
7 mM cRGDfC 10 kPa (our highest performing PEG hydrogel)	82	

Table 1. Comparison of synthetic substrates and our PEG hydrogels' performance in iPSC-CM differentiation efficiency.

	cTnT expression (%)	Variability across experiments	Variability across replicates
Matrigel	60	25.3	6.2
PEG hydrogels	75	8.2	3.5
Difference	↑ 25 %	↑ 65 %	↑ 45 %

Table 2. Summary comparison of Matrigel and PEG hydrogel performance in iPSC-CM differentiation efficiency.

Data availability statement

The data supporting this article have been included as part of the Supplementary Information.